This file contains all reviewer reports in order by version, followed by all author rebuttals in order by version.

nature portfolio

Peer Review File

Magnetic Localization and Manipulation of Locking Synchronous Motors

Corresponding Author: Professor Sarthak Misra

Version 0:

Reviewer comments:

Reviewer #1

(Remarks to the Author)
The manuscript demonstrates a device capable of magnetic localization and manipulation. The two modes can be switched by a low melting point alloy activated by resistant-induced heating. The manuscript investigates and validates the devices from fabrication, tracking performance, and validations with predefined trajectories and a simple phantom platform. The results are thorough and inspiring for the community of biomedical device tracking. However, there are a lot of major issues need to be improved before its publication.
Major points:
1. Why is ferrofluid bearing used in the device? The resistance needs to be characterized and compared with other solid bearings, e.g. in the Ref 60, and other fluidic bearings.
2. Since the fabrication is complicated, the fabrication process presented in Figure 2a is better to use cross-sectional views.
3. In content relative to Figure 3c, the authors demonstrated the feasibility of the heating of the alloy for unlocking the motor with respect to room temperature. Since the device is expected to use in human body, have they considered testing the heating performance with respect to body temperature (37degC)? And how about the cooling process? With body temperature, the cooling process will be slower so that the switching between the locking and unlocking mode will be prolonged. What is the achievable switching frequency between the two modes?
4. What is the expected application of the PMSM method? It is hinted that it can be used for intravascular catheter, however, detailed introduction and discussions are necessary.
5. For magnetic field modeling, why did the authors choose a finite-element-informed multipole expansion model? Does the magnetic field generated by the driving coils affect the localization accuracy or frequency?
6. The definitions of the field's rotation axis and the rotor's magnetization axis are hard to imagine based on the illustration in Figure 4d and description in line 175.
7. Why the b_ratio is varying between 1 and 2 as shown in Figure 4f?
8. The authors mentioned that the algorithm finds four non-unique solutions of the beta angle, how did they determine the unique pose?
9. What is the distance from the device to the sensor for the tracking in Figure 7?
Minor points:
1. The authors used a lot of lines for labeling with gradient colors. However, due to the gradient effects on lines with different lengths, e.g. in Figure 2a, the lines labeling the same item show different colors which make the labeling confusing. Please be careful with the targeting location of the illustration, e.g. the lines for the adhesive do not indicate the correct layer.
2. It is better to label the process with steps (i) to (vi) and indicate them in the text (paragraph 2 of the Permanent magnet synchronous motor section) for clearer demonstration.
3. The colors of the axes in Figure 2b to 2d should be consistent and how about the axes in Figure 2d?

Reviewer #2

(Remarks to the Author)
This article proposes a novel magnetic localization method for magnetic manipulation and localization systems. This method uses a single external tri-axial magnetometer to measure the internal rotating dipole field generated by the permanent magnet synchronous motor (PMSM) rotor for localization. The PMSM is composed of a permanent magnet (PM) rotor, two stator coils for PM rotation, and low melting point alloy (LMPA) for PM locking. Specifically, The LMPA's phase transition lock or unlock the PM rotor, enabling mode switching between localization and manipulation. The system is validated through localization experiments and a manipulation and localization experiment inside a tubular vessel.

Overall, the innovative PMSM design facilitates a compact system structure, successfully integrating magnetic localization and manipulation into the system. However, it needs some revisions that could enhance the technical soundness of the article.

1. From the Video S1 “Rotor rotation at different frequencies”, the PM rotation seems to exhibits eccentricity. This could introduce offsets in the motor rotation axis ωˆ_m which should ideally remain constant in a single rotation axis. This potentially leads to tracking errors. The article would benefit from a discussion of possible solutions, both in terms of hardware and algorithmic approaches.

2. Is the magnetic field generated by the stator (coils) detectable for the external magnetometer, will this affect the localization?

3. Typical magnetic localization uses nonlinear optimization or state estimation based on a straight-forward magnetic measurement model to acquire pose estimation. This article, however, analyzes the rotation process using rotor field isoline functions and fits isoline functions for key variables (_^s)β, (_^s)p_e , and (_^s)α, which could be a unique contribution of this work. It would be beneficial to further discuss how this parameterization and function fitting benefit the system, as well as how this algorithm compares to conventional methods in other rotating dipole systems. Additionally, the tracking errors in this system appear to be slightly larger than those observed in similar rotating dipole localization systems, and this system has a smaller workspace. Is the algorithm responsible for this discrepancy?

4. In Figure 6, the position estimation results show a large error peak when the position angle $\beta > 70°$. This is a well-known phenomenon in single magnetic source systems, often referred to as a singularity or low-sensitivity issue, as reported in [1][2]. The article could benefit from referencing these relevant works. However, the error peaks around $\beta = 23°$ is not well-discussed. Considering the system’s operating scenario, $\beta \approx 23°$ is a commonly encountered workspace, and significant orientation error (error in ωˆ_m) should be discussed in more details.

[1] A. Z. Taddese, P. R. Slawinski, M. Pirotta, E. De Momi, K. L. Obstein, and P. Valdastri, “Enhanced real-time pose estimation for closed-loop robotic manipulation of magnetically actuated capsule endoscopes,” The International Journal of Robotics Research, vol. 37, no. 8, pp. 890–911, Jul. 2018
[2] Y. Shen, S. Dong, D. Liu, K. Zhang, and H. Wang, “Active 6-DoF Electromagnetic Pose Tracking Using Orientation Control of the Magnetic Source,” 2023 IEEE International Conference on Robotics and Biomimetics (ROBIO), Koh Samui, Thailand: IEEE, Dec. 2023, pp. 1–7.

5. In the manipulation and localization experiments, the use of additional tri-axial magnetometers seems acceptable, as the external space is not confined. Adding one to three more magnetometers will help the system determine a unique solution without compromising its compact configuration.

6. Typically, the Hall-effect magnetometer has limitations in terms of sensitivity and resolution, which may impact the system's accuracy. Additionally, the resolution and sensory noise are needed to be listed in the article.

7. The system in this article does not appear to be a strictly simultaneous magnetic manipulation and localization system. Therefore, the phase transition or mode-switching time becomes a critical factor for its efficiency. Are there any modifications that could accelerate this process? Why are sinusoidal currents used to drive the stator coils, given that DC currents would typically provide higher power output, when activating the rotating PM? Additionally, LMPA solidification time should also be experimentally tested and discussed.

8. Is there a specific design in place to prevent the liquidized alloy from leaking? While the article discusses the safety of the LMPA melting temperature, it would be helpful to briefly address the design considerations for preventing leaks and potential hazards associated with the LMPA to the human body.

Reviewer #3

(Remarks to the Author)
I found this to be a quite interesting paper and design concept/paradigm. The authors make a kind of robotic guidewire that effectively has a tiny brushless motor in its tip. Using this motor, they can rotate the permanent-magnet rotor via the electromagnetic stator, and then pick up this rotating dipole field using Hall-effect sensors (which would be located outside of the patient's body in practice). This localization is used while traversing vasculature. Since the Hall-effect sensors are on a system outside of the body, it is reasonable to assume that the Earth's magnetic field can be calibrated away, enabling measurement of very small fields. If magnetic steering is needed, such as to select a branch at a given branch point, then a ferrofluid bearing is allowed to solidify, stopping the rotating-magnet localization function, but enabling traditional magnetic-tip steering using an external magnetic-actuation system (which is now being done blind, but over a tiny workspace). Once steering is complete, the ferrofluid is melted using induction (using the same stator coils) and the rotating-magnet localization can begin again. The authors include a number of clarifying videos that help the reader understand what is happening.

There is a lot of prior work on doing localization using rotating magnetic dipole fields. I find the literature search largely sufficient. However, it is often unclear what developments regarding localization using rotating magnetic dipoles are newly developed here, and what has already appeared in the literature. References to the literature are largely isolated to the Introduction. Also, there are two uncited papers that are also about localization using a rotating magnetic dipole (although, by contrast, the place sensors inside the body):

Popek et al.,, "First Demonstration of Simultaneous Localization and Propulsion of a Magnetic Capsule in a Lumen using a Single Rotating Magnet", IEEE International Conference on Robotics and Automation, pp. 1154-1160, 2017.

Sperry et al., "Six-degree-of-freedom Localization with a 3-axis Accelerometer and a 2-axis Magnetometer for Magnetic Capsule Endoscopy", IEEE Robotics and Automation Letters, 7:2110-2115, 2022.

Early in the paper, the authors mention that it is not possible to uniquely localize a rotating magnetic dipole (i.e., the 3-dof position and the axis of rotation) using a single ori-axial Hall-effect sensor, and one can only narrow it down to four possible locations. But then later, they seem to show a unique localization. This discrepancy is only resolved at the end of the paper. My suggestion would be to clarify this earlier in the paper, so the reader isn't left hanging and dwelling on this.

One problem that I have with this paper is that it is not very constructive. If I wanted to apply this method to my own problem, it would take substantial effort to reconstruct it. The authors provide all of the pieces, but don't really connect the dots very well. Figure 5 is close to what I'm looking for. Maybe the authors could expand on that content in a narrative fashion (even in Supplementary Material).

When the magnetic tip is solidified, the magnetization is diametric (not axial), but I guess it can assumed to be known (at least approximately) based on the last stator commands. However, the localization of the stator, in the roll direction, is likely poorly known, as with all of this type of long, continuum device. I was left wondering how that affected the subsequent steering. For example, I could imagine that the first time the external electromagnet is turned on, it would be difficult to even anticipate what direction the tip would bend in, and it would be almost random. Can you please clarify this aspect of the method.

I like the "future work" suggestion that this device could be used as an in-vivo rotating dipole field source. That's an interesting idea.

I was left with questions of scalability. For the device to get even a little smaller, the fabrication of the stator would become more difficult, and probably more importantly, the permanent-magnet rotor would decrease in size, and its field (which is proportional to its volume) would decrease drastically, maybe below the point of being measurable by external Hall-effect sensors. Maybe this device is already small enough for useful tasks?

Version 1:

Reviewer comments:

Reviewer #1

(Remarks to the Author)
The authors have revised the manuscript according to the reviewers comments. The paper is ready for publication.

Reviewer #2

(Remarks to the Author)

Thank you for your detailed responses. The issues raised in my previous comments have been well addressed with satisfactory revisions. I recommend the publication of this paper after incorporating the following minor comments.

1. For the previous comment 4 about Figure 6 and experimental results, I appreciate the detailed and sound error analysis provided for the unexpected errors occurring at $\beta \leq 23\circ$.

While I understand the cause of this unexpected error is complicate and difficult to isolate, a hypothesis on the potential cause would be useful and could help enlighten readers. However, regarding the statement in line 266-267 “Therefore, it may be related to a problem with our sensor…”, It’s not clear how the general sensor problem is directly linked to regional low accuracy. I would suggest reconsidering this claim, either by removing it or providing a more thorough explanation.

2. Regarding the previous comment on the use of sinusoidal currents to drive the stator coils in the heating process (previous comment 7), I understand PMSM use AC current to generate the rotating magnetic field. I was wondering about the potential of using DC current exclusively during the heating process (e.g. 0~30s in Fig. 3 (g)) to accelerate the melting process, enhancing the real-time performance of the system. I guess that it is because switching to DC current in heating process requires more complex power circuit design.

Reviewer #3

(Remarks to the Author)
I am satisfied with the authors' improvements to the manuscript. They haven't solved every problem yet, but this paper makes an interesting contribution to the literature.

Version 2:

Reviewer comments:

Reviewer #2

(Remarks to the Author)
The manuscript is ready for publication now.

Authors' response to the reviewers' comments

Manuscript ID: COMMSENG-24-0654A

Magnetic Localization and Manipulation of Locking Synchronous Motors

Authors: Michiel Richter, Lukas Masjothusmann, Pavlo Makushko,
Venkatasubramanian Kalpathy Venkiteswaran, Denys Makarov, Sarthak Misra

Reviewer 1

The manuscript demonstrates a device capable of magnetic localization and manipulation. The two modes can be switched by a low melting point alloy activated by resistant-induced heating. The manuscript investigates and validates the devices from fabrication, tracking performance, and validations with predefined trajectories and a simple phantom platform. The results are thorough and inspiring for the community of biomedical device tracking.

Response: We appreciate the reviewer's positive remarks about the manuscript, as well as the detailed review.

However, there are a lot of major issues need to be improved before its publication. Major points:

1. *Why is ferrofluid bearing used in the device? The resistance needs to be characterized and compared with other solid bearings, e.g. in the Ref 60, and other fluidic bearings.*

   Response: We agree that the first mention of a ferrofluid bearing in the results section is abrupt and unsupported.

   Indeed, ferrofluid bearings are but one of the possible bearings among others, including dry-film lubricants [A], jewel bearings [B], and micro-ball bearings [C]. The ferrofluid bearing is included as an antifriction mechanism inspired from other works [D,E,F] on small-scale permanent magnet synchronous motors (PMSMs). However, we do believe that a characterization of resistance and comparison with other solid and fluidic bearings falls outside the scope and intended purpose of the manuscript. Rather, our intention is to present the idea of reversible locking of the rotor, and interpretation of its rotating field for localization and informed field generation towards magnetic manipulation.

   We acknowledge that these works warrant citation and that the introduction of the manuscript should mention the ferrofluid bearing. Accordingly, we have made the following changes to the manuscript.

   - Introduction (lines 66-69): Mention that a ferrofluid bearing is added to address friction losses due to electromagnetic attraction forces between stator and rotor. Also added that ferrofluid bearings have been used in other small-scale PMSMs with new references [D][E][F] as low-cost and complexity alternatives to dry-film lubricants [A], jewel bearings [B], or micro-ball bearings [C].

   [A](49) Bandorf, R. et al. Different carbon based thin films and their microtribological behaviour in mems applications. Surf. Coat. Technol. 200, 1777–1782 (2005).

   [B](50) Wang, T. et al. Development of a high-speed synchronous micro motor and its application in intravascular imaging. Sens. Actuator A Phys. 218, 60–68 (2014).

   [C](51) Ghalichechian, N., Modafe, A., Beyaz, M. I. & Ghodssi, R. Design, fabrication, and characterization of a rotary micromotor supported on microball bearings. J. Microelectromech. Syst. 17, 632–642 (2008)

   [D](46) Assadsangabi, B., Tee, M. & Takahata, K. Ferrofluid-assisted levitation mechanism for micromotor applications. In 2013 Transducers & Eurosensors XXVII: The 17th International Conference on Solid-State Sensors, Actuators and Microsystems (TRANSDUCERS & EUROSENSORS XXVII), 2720–2723 (IEEE, 2013).

   [E](47) Assadsangabi, B., Tee, M. H., Wu, S. & Takahata, K. Catheter-based microrotary motorenabled by ferrofluid for microendoscope applications. J. Microelectromech. Syst. 25, 542–548 (2016)

   [F](48) Jayhooni, S. M. H., Assadsangabi, B. & Takahata, K. A stepping micromotor based on ferrofluid bearing for side-viewing microendoscope applications. Sens. Actuator A Phys. 269, 258–268 (2018).

2. *Since the fabrication is complicated, the fabrication process presented in Figure 2a is better to use cross-sectional views.*

   Response: We thank the reviewer for the suggestion on improving the clarity of the fabrication process by providing cross-sectional views. Since Figures 2a and 2b both show external views of the PMSM, we believe that presenting cross-sectional views of the fabrication steps as supplementary information would maintain coherence between structural representations. Accordingly, the following changes have been made to the manuscript.

- Supplementary Material: Added a new figure, Fig. S2 (also shown below), that details the non-cross-sectional and cross-sectional views side by side.
- Results (line 97-98): Added a reference to supplementary figure 2 for cross-sectional views of fabrication steps.

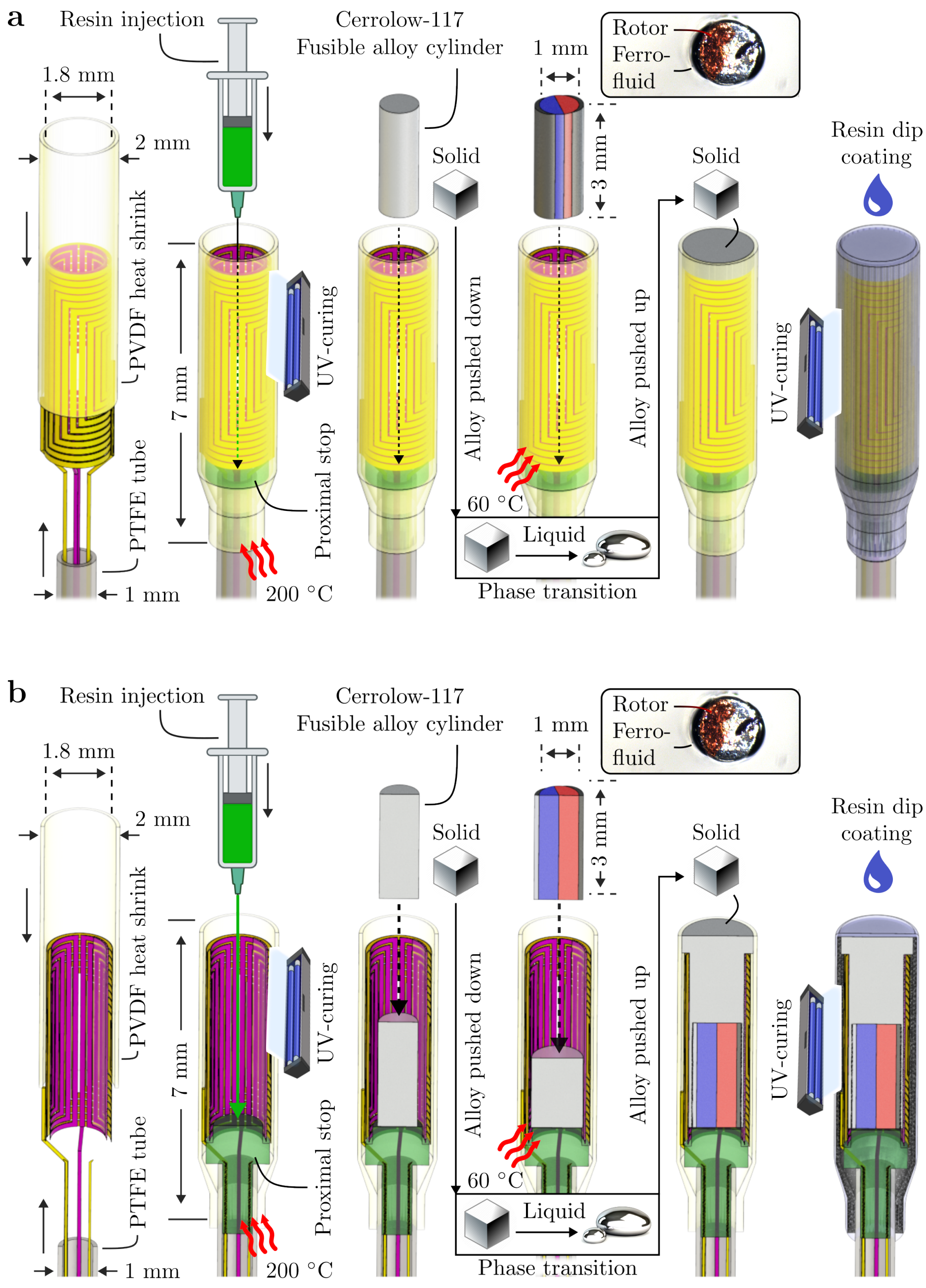

Fig. S2: **Fabrication process of the permanent magnet synchronous motor. a** Non-cross-sectional view of fabrication steps. **b** Cross-section view showing internal arrangements of components.

3. *In content relative to Figure 3c, the authors demonstrated the feasibility of the heating of the alloy for unlocking the motor with respect to room temperature. Since the device is expected to use in human body, have they considered testing the heating performance with respect to body temperature (37degC)? And how about the cooling process? With body temperature, the cooling process will be slower so that the switching between the locking and unlocking mode will be prolonged. What is the achievable switching frequency between the two*

modes?

Response: Temperature measurements were performed in air to match conditions for further characterizations such as rotor unlocking, as well as be representative of the environment during the demonstrations of localization and manipulation. However, we agree that due to the medical context of the demonstrations, heating and cooling of the motor should also be tested with respect to body temperature. To this end, we have repeated the temperature measurements in both air (18degC) and heated water (37degC), and visualized the results in an updated Figure 3c (also shown below).

Based on the new measurements, heating and cooling occurs faster in water than in air, with similar internal steady-state temperature (50degC). Surface temperature rises less in water (37-40degC) than in air (18-31degC). The system reaches steady-state in 20 s in water and 45 s in air, while passive cooling below the transition temperature takes just 2 s. This is indicative of the rate for switching between PMSM localization and manipulation modes.

Based on the reviewer's comments, the new experimental data, and above discussion, the following changes are made to the manuscript:

- Figure 3c: Replaced with new subfigure (shown below) containing internal and external motor temperatures in air and water. Updated the caption.
- Supplementary Figure 3: Replaced with a new figure (shown below) containing the experimental setups for temperature experiments in air and water.
- Results (line 118-126): Updated results to include temperature measurements in water.
- Discussion (line 336-342): Included discussion on heating and cooling times with the relation to switching rate between localization and manipulation modes.

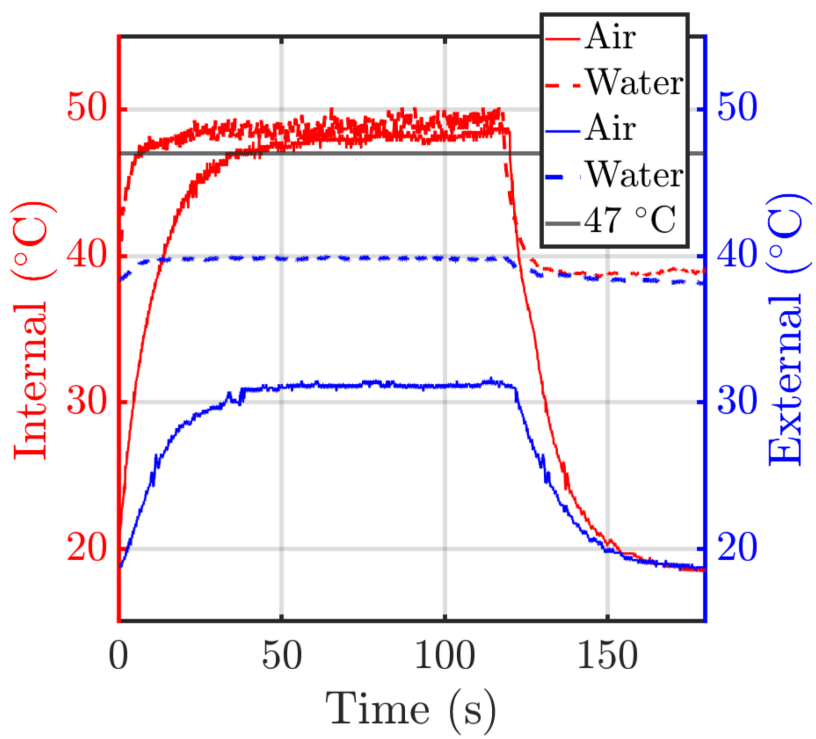

Figure 3: Updated figure 3c. Measured internal and surface temperatures from 200 mA quadrature currents in room-temperature air (18 °C) and heated water (37 °C)

4. *What is the expected application of the PMSM method? It is hinted that it can be used for intravascular catheter, however, detailed introduction and discussions are necessary.*

Fig. S3: **Temperature measurements. a** External temperature measurement inside a bath of distilled water at 37 °C. Visible are the motor with outer stator and resin shell, but without the permanent magnet rotor, and a thermocouple placed along its outer surface. **b** Internal temperature measurement inside a bath (glass jar) of distilled water at 37 °C. The thermocouple is placed inside the motor's rotor cavity. The water is heated with a hot plate. **c** Internal temperature measurement inside air at 18 °C.

Response: The PMSM represents a rotating magnetic dipole with perpendicular magnetization and rotation axes. The presented application of the PMSM is three-dimensional localization based on field measurements, informing reconfiguration of a magnetic manipulation system for targeted field generation. Nevertheless, the localization method is compatible with any structure that incorporates such a rotating dipole.

We have made the following changes to the manuscript to clarify the above discussion:

- Introduction (line 74-76): Rephrasing to emphasize that the PMSM is able to switch between unlocked rotor state (localization mode) and locked rotor state (manipulation mode).
- Discussion (line 345-346): Noted that the presented algorithm localizes a PMSM, modeled as a magnetic dipole with perpendicular rotation and magnetization axes.

5. *For magnetic field modeling, why did the authors choose a finite-element-informed multipole expansion model? Does the magnetic field generated by the driving coils affect the localization accuracy or frequency?*

Response: Our goal was to develop an accurate 3D field model of a diametrically magnetized cylindrical permanent magnet rotor. This model is necessary for formulating the rotor field isoline functions, which are central to the localization algorithm. To have a model be as accurate as possible, it needs to conform to Maxwell's equations in current-free space, i.e. the model needs to be divergence- and curl-free.

Options for analytical field models are the dipole approximation and the multipole expansion model. Notably, the dipole approximation is the first-order term in the multipole expansion model, with reduced accuracy close to the magnetic field source [A]. On the other hand, the multipole expansion model contains coefficients that require optimization through model fitting to reference field data. To obtain accurate 3D reference field data, we used a measurement-informed scaled finite-element (FE) model. The reason we did not solely rely on the FE model, is that its estimations contain (small) fluctuations do not enforce the divergence- and curl-free properties of magnetic fields.

The magnetic field generated by the driving coils are considered negligible regarding localization accuracy and frequency. This, because its field is one to two orders weaker than that of the rotor. The field strength of the stators does determine the maximum rate of rotor rotation, and thereby affects the achievable localization frequency.

The localization frequency depends on rate of rotor rotation, sensor sampling frequency, the number of samples, and computation time. Higher localization frequencies can be achieved using faster sampling, reducing number of samples (speeding up measurement time and data processing). In combination, the rotor rotation rate could be increased, which was shown up to 10 Hz. Faster rotor rotation rates may be achieved by increasing the current through the stators.

To address the above discussion, the following changes have been made to the manuscript:

- Figure 3d: Added rotor field estimations from a point dipole model to compare to field measurements and estimations of a finite element model [A].
- Results (line 135-136): Added that 1D measurements are compared to a point dipole approximation, and mention that the 1D measurements are used to scale a numerical 3D finite element model.
- Results (line 192-198): Added a paragraph to note and explain that the magnetic field of the stators is ignored during formulation of the isoline functions. Also contains a reference to a new supplementary figure S6.
- Supplementary Material: Added new figure S6 (shown below) that quantifies and compares the magnetic field of the stator to that of the rotor.
- Discussion (line 395-401): Added a paragraph specific to a discussion on localization frequency.

[A](55) Petruska, A. J. & Abbott, J. J. Optimal permanent-magnet geometries for dipole field approximation. IEEE Trans. Magn. 49, 811–819 (2012)

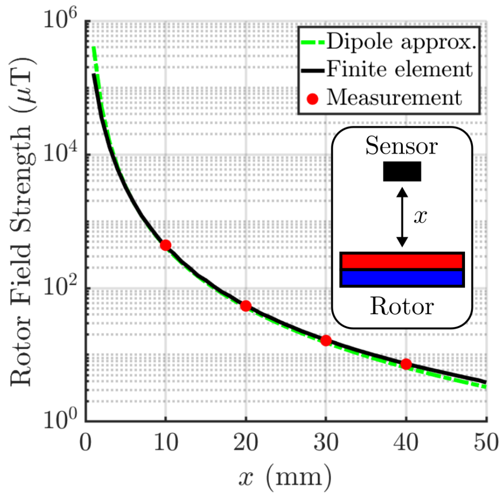

Figure 4: Updated figure 3d. Added line "Dipole approx."

6. *The definitions of the field's rotation axis and the rotor's magnetization axis are hard to imagine based on the illustration in Figure 4d and description in line 175.*

   Response: Indeed, simplification from 3D to 2D is paired with loss of information required for interpretation. Figure 4d was made in 2D as to simplify definitions of vectors and angles, but indeed loses the third dimension that contains out-of-plane vectors necessary to visualize the rotating field vectors and their axis of rotation. Accordingly, we have made the following changes to the manuscript:

   - Supplementary Material: Added new supplementary figure 5 (shown below), that illustrates a 3D representation of rotor rotation and the resulting rotating fields with elliptically varying field strength.

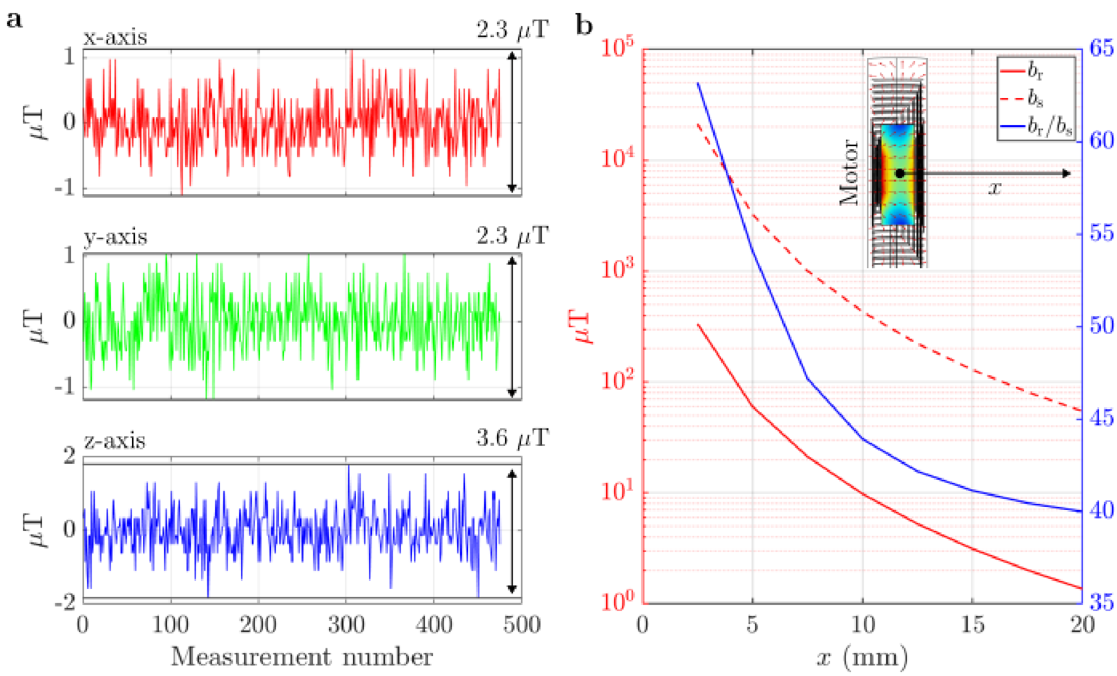

Fig. S6: **Hall effect sensor noise and comparison between magnetic fields of the rotor and stator. a** Noise signal of the Hall effect sensor obtained from a mean-correction of static background field measurements. **b** Finite element simulated magnetic fields of the permanent magnet rotor (b_r) and electromagnet stator (b_s), corrected for driving current (200 mA). In addition, the ratio between rotor and stator fields (b_r/b_s) is shown.

- Results (line 171, 181): Added references to the new supplementary figure 5 to complement figure 4d.
- Figure 4d: Added a reference to the new supplementary figure within the caption.

7. *Why the b_ratio is varying between 1 and 2 as shown in Figure 4f?*

   Response: This is a property of rotating magnetic fields generated by a rotating dipole with perpendicular magnetization and rotation axes. It can be demonstrated with the magnetic point dipole approximation. For a point dipole with perpendicular magnetization and rotation axes, the field strength remains constant for positions along the rotation axis (b_ratio is 1). In contrast, for positions that cyclically align with the magnetization axis, the field strength varies by a factor of two (b_ratio is 2). According to the simulations with our multipole expansion model (including a dipole model), any other positions will experience a field strength that varies by a factor between 1 and 2. To address the reviewer's comment, we have made the following changes to the manuscript:

   - Supplementary Material: Added a new text section (Supplementary Text 1, shown below), that derives the maximum bound of the field ratio by using the point dipole approximation.
   - Results (line 188): Added a reference to Supplementary Text 1 after mentioning Figure 4f that illustrates that the field ratio is cyclic and bounded between 1 and 2.

8. *The authors mentioned that the algorithm finds four non-unique solutions of the beta angle, how did they determine the unique pose?*

   Response: Indeed, based on single-sensor measurements of magnetic fields generated by a rotating dipole, there are four possible solutions for the combination of position and rotation axis of the dipole. To determine a unique solution, it is possible to either use more sensors, or (what we have done) use feedback of a previously reconstructed PMSM position. The latter requires at least the starting pose of the PMSM to be known. We have made the following adjustments to the manuscript.

   - Introduction (line 60-62): Added that in this study, the fourfold ambiguity is resolved using a-priori knowledge of the rotating dipole position, obtained with closed-loop position feedback.

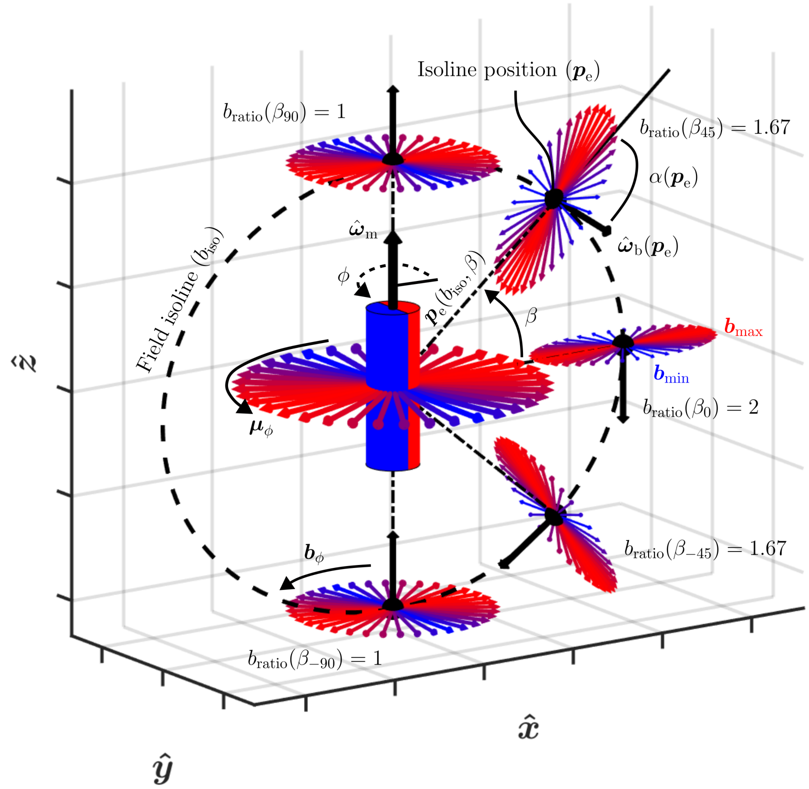

Fig. S5: **A 3D representation of a rotating magnetic dipole (rotor magnet) with perpendicular magnetization and rotation axes.** The magnet has rotation axis ($\hat{\boldsymbol{\omega}}_m$) and rotation angle ($\phi$), that orient the rotating dipole moment ($\boldsymbol{\mu}_\phi$). During magnet rotation, at any position in space, the field ($\boldsymbol{b}_\phi$) rotates in-plane with a field rotation axis ($\hat{\boldsymbol{\omega}}_b$). The field has an elliptically varying field strength between maximum ($\boldsymbol{b}_{max}$) and minimum ($\boldsymbol{b}_{min}$) values, with an associated field ratio ($b_{ratio} = \|\boldsymbol{b}_{max}\|/\|\boldsymbol{b}_{min}\|$). Within the magnetization plane of the magnet, spanned by $\hat{\boldsymbol{\omega}}_m$ and $\hat{\boldsymbol{\mu}}_0$, a field isoline ellipse is defined of constant field strength (b_{iso}). Each position on the ellipse, termed the isoline position ($\boldsymbol{p}_e(b_{iso}, \beta)$), depends on b_{iso} and an isoline position angle ($\beta = \angle \boldsymbol{p}_e, \boldsymbol{\mu}_0$). Then, each $\boldsymbol{p}_e(b_{iso}, \beta)$ is associated with field vectors of maximum strength ($\boldsymbol{b}_{max}(\boldsymbol{p}_e)$), minimum strength ($\boldsymbol{b}_{min}(\boldsymbol{p}_e)$), and rotation ($\hat{\boldsymbol{\omega}}_b(\boldsymbol{p}_e)$), as well as scalars of field ratio ($b_{ratio}(\boldsymbol{p}_e)$) and field angle ($\alpha(\boldsymbol{p}_e) = \angle \boldsymbol{p}_e, \hat{\boldsymbol{\omega}}_b(\boldsymbol{p}_e)$).

- Results (line 190-191): Added that in this work, the ambiguity is resolved using closed-loop feedback of previous localizations, with reference to equation (14) and explanatory figure 8d.
- Discussion (line 352-354): Added a paragraph that the fourfold ambiguity is also found in similar work [A]. Also, that we resolved this using prior knowledge of dipole position, with a risk of forwarding a previous faulty localization.
- Materials and Methods (line 606-607): Noted that the initial position was provided to the localization algorithm.

9. *What is the distance from the device to the sensor for the tracking in Figure 7?*

Response: In Figure 7, the axis-specific and total motor-to-sensor distances are shown in the left panels with $\boldsymbol{p}_m = \langle p_{m,x}, p_{m,y}, p_{m,z} \rangle$. We agree that this can be better defined. Accordingly, we have made the following changes:

- Results (line 271): Added a mention that predetermined positions and rotation axes for tracking are with respect to the sensor.
- Results (line 277): Added an explicit mention of reporting sensor-to-motor distances.
- Figure 7: Added to the caption that tracking results are with respect to the sensor frame.

Minor points:

1. *The authors used a lot of lines for labeling with gradient colors. However, due to the gradient effects on lines with different lengths, e.g. in Figure 2a, the lines labeling the same item show different colors which make the labeling confusing. Please be careful with the targeting location of the illustration, e.g. the lines for the adhesive do not indicate the correct layer.*

   Response: We have changed the lines with gradient effects to uniform colors. Also, we thank the reviewer for spotting our error on labeling the adhesive layer. The corresponding line now correctly labels the adhesive layer.

2. *It is better to label the process with steps (i) to (vi) and indicate them in the text (paragraph 2 of the Permanent magnet synchronous motor section) for clearer demonstration.*

   Response: We thank the reviewer for the suggestion to improve the clarity of figure 2a. Upon revision of our manuscript, we noticed that paragraph 1 of the Permanent magnet synchronous motor section already described the main components of the PMSM, and that paragraph 2 would be superfluous to a more detailed caption of the figure in combination with the explicit fabrication process described in the Materials and Methods section. We have made the following changes:

   - Figure 2: Added labels (i)-(vii) to the different steps in the fabrication process. Modified the caption to individually discuss the different labeled steps.
   - Results (Permanent magnet synchronous motor section): Removed paragraph 2. Added a reference to figure 2a in paragraph 1, connecting to the updated caption with labels.

Supplementary Text 1 – Field ratio of rotating dipoles

Given the magnetic point dipole approximation, defined as

$$\boldsymbol{b}(\boldsymbol{p}) = \frac{\mu_0}{4\pi}\left(\frac{3\boldsymbol{p}(\boldsymbol{\mu}\cdot\boldsymbol{p})}{\|\boldsymbol{p}\|^5} - \frac{\boldsymbol{\mu}}{\|\boldsymbol{p}\|^3}\right), \tag{1}$$

where $\boldsymbol{b}(\boldsymbol{p}) \in \mathbb{R}^3$ is the magnetic field at some position ($\boldsymbol{p} \in \mathbb{R}$), and $\boldsymbol{\mu} \in \mathbb{R}^3$ is the dipole moment. Consider that the dipole is rotating, and that $\boldsymbol{\mu}$ is perpendicular to the rotation axis ($\hat{\boldsymbol{\omega}}$). We define an angle of rotation ($\phi \in [0, 2\pi)$, let the dipole's rotation axis be its local z-axis ($\boldsymbol{\omega} = \hat{\boldsymbol{z}}$), and define the rotated dipole moment as $\boldsymbol{\mu}_\phi = \boldsymbol{R}_z(\phi)(\mu\hat{\boldsymbol{x}})$.

The field is maximum when $\boldsymbol{\mu}$ and $\boldsymbol{p}$ are parallel, i.e. for $\boldsymbol{\mu}_0 = \mu\hat{\boldsymbol{x}}$ and $\boldsymbol{p} = p\hat{\boldsymbol{x}}$,

$$\begin{aligned}\boldsymbol{b}_{\max}(\boldsymbol{p}) &= \frac{\mu_0}{4\pi}\left(\frac{3p\hat{\boldsymbol{x}}(\mu\hat{\boldsymbol{x}}\cdot p\hat{\boldsymbol{x}})}{p^5} - \frac{\mu\hat{\boldsymbol{x}}}{p^3}\right) &(2)\\ &= \frac{\mu_0}{4\pi}\left(\frac{3p^2\mu\hat{\boldsymbol{x}}(\hat{\boldsymbol{x}}\cdot\hat{\boldsymbol{x}})}{p^5} - \frac{\mu\hat{\boldsymbol{x}}}{p^3}\right) &(3)\\ &= \frac{\mu_0}{4\pi}\left(\frac{2\mu}{p^3}\right)\hat{\boldsymbol{x}}. &(4)\end{aligned}$$

Conversely, the field is minimum when $\boldsymbol{\mu}$ and $\boldsymbol{p}$ are perpendicular, i.e. for $\boldsymbol{\mu}_{\pi/2} = \mu\hat{\boldsymbol{y}}$ and $\boldsymbol{p} = p\hat{\boldsymbol{x}}$,

$$\boldsymbol{b}_{\min}(\boldsymbol{p}) = \frac{\mu_0}{4\pi}\left(-\frac{\mu}{p^3}\right)\hat{\boldsymbol{y}}. \tag{5}$$

Therefore, the ratio between the maximum and minimum field strength, for a rotating dipole, is at most two,

$$b_{\text{ratio}} = \frac{\|\boldsymbol{b}_{\max}(\boldsymbol{p})\|}{\|\boldsymbol{b}_{\min}(\boldsymbol{p})\|} = 2. \tag{6}$$

- Methods (Assembly of the PMSM section, line 390): Added references to figure 2a(i)-(vii) within the description of the fabrication process.

3. *The colors of the axes in Figure 2b to 2d should be consistent and how about the axes in Figure 2d?*

   Response: We have changed the colors of the axes to be the same across the subfigures, and added a set of axes to figure 2d.

Reviewer 2

This article proposes a novel magnetic localization method for magnetic manipulation and localization systems. This method uses a single external tri-axial magnetometer to measure the internal rotating dipole field generated by the permanent magnet synchronous motor (PMSM) rotor for localization. The PMSM is composed of a permanent magnet (PM) rotor, two stator coils for PM rotation, and low melting point alloy (LMPA) for PM locking. Specifically, The LMPA's phase transition lock or unlock the PM rotor, enabling mode switching between localization and manipulation. The system is validated through localization experiments and a manipulation and localization experiment inside a tubular vessel.

Overall, the innovative PMSM design facilitates a compact system structure, successfully integrating magnetic localization and manipulation into the system.

Response: We appreciate the reviewer's remarks, which we used to revise the manuscript.

However, it needs some revisions that could enhance the technical soundness of the article.

1. *From the Video S1 "Rotor rotation at different frequencies", the PM rotation seems to exhibits eccentricity. This could introduce offsets in the motor rotation axis ω_m which should ideally remain constant in a single rotation axis. This potentially leads to tracking errors. The article would benefit from a discussion of possible solutions, both in terms of hardware and algorithmic approaches.*

   Response: Video S1 shows rotation of the permanent rotor in an otherwise empty rotor cavity of the motor. Eccentricity occurs due to magnetic attraction to the stator. To mitigate this effect and prevent friction, ferrofluid bearings have been used in small-scale permanent magnet linear and rotary motors [A][B][C]. Similarly, we incorporated a ferrofluid bearing to minimize eccentricity. However, its first mention appears abruptly in the results section without prior context. Additionally, Video S1 does not include the ferrofluid bearing.

   During eccentric rotor rotation, its position shifts but its axis of rotation remains unchanged. We agree that such a shift can alter the maximum and minimum field strengths and their ratio, potentially leading to tracking errors. The impact of these errors depends on the rotor's field gradients at a given measurement position (Fig. 3f).

   Based on the potential air gap of our motor, the rotor position can shift radially by approximately 0.1 mm. Based on the rotor's field gradients along its magnetization axis, this shift would cause a field change of 0.8 μT (relative to a 55 μT field) at a 20 mm distance and 0.05 μT (relative to 7 μT) at 40 mm. This suggests that the effect of rotor eccentricity diminishes with increasing distance from the measurement position and may be considered negligible. This is a result of field gradients diminishing faster with distance than field strengths.

   To address the reviewer's comment, we have made the following changes to the manuscript:

   - Introduction (line 66-67): Added that a ferrofluid bearing is used as an antifriction mechanism that also ensures concentricity of the rotor and stator. Reference uses of ferrofluid bearings in other small-scale motors [A][B][C].
   - Supplementary Video S1: Added new recordings of rotor rotation with a ferrofluid bearing.
   - Figure 1a: Added a label to indicate a ferrofluid bearing.
   - Discussion (line 325-327): Noted that the ferrofluid bearing is used to minimize friction, oppose magnetic attraction between stators and rotor, and maintains concentricity during rotation.
   - Discussion (line 389-390): Added that as a potential source of error in localization accuracy, the micrometer-range eccentricity during rotor rotation is considered negligible due to its near-zero field gradient.

[A](46) Assadsangabi, B., Tee, M. & Takahata, K. Ferrofluid-assisted levitation mechanism for micromotor applications. In 2013 Transducers & Eurosensors XXVII: The 17th International Conference on Solid-State Sensors, Actuators and Microsystems (TRANSDUCERS & EUROSENSORS XXVII), 2720–2723 (IEEE, 2013).

[B](47) Assadsangabi, B., Tee, M. H., Wu, S. & Takahata, K. Catheter-based microrotary motorenabled by ferrofluid for microendoscope applications. J. Microelectromech. Syst. 25, 542–548 (2016)

[C](48) Jayhooni, S. M. H., Assadsangabi, B. & Takahata, K. A stepping micromotor based on ferrofluid bearing for side-viewing microendoscope applications. Sens. Actuator A Phys. 269, 258–268 (2018).

2. *Is the magnetic field generated by the stator (coils) detectable for the external magnetometer, will this affect the localization?*

Response: We assumed the stator field to be negligible compared to that of the rotor. However, this warrants further analysis to validate.

First, new finite-element simulations of the stator field strength indicate a one to two-order difference with the rotor field. Also, measurements of the sensor's noise signal indicate that the stator field drops below distinguishable values beyond 15 mm distance.

Second, under the assumption of synchronous rotation of the rotor's magnetization axis with the stator field, we may consider that the stator acts to amplify the rotor's magnetic moment. In that case, although the field strengths ($\{b_{\max}, b_{\min}\},\ b_* := \|\boldsymbol{b}_*\|$) shift for some position in space, its $\{b_{\text{ratio}}, \hat{\boldsymbol{b}}_{\min}, \hat{\boldsymbol{\omega}}_{\text{b}}\}$ does not. Since $\|\boldsymbol{p}_{\text{e}}\|$ depends on $b_{\text{iso}} \equiv b_{\max}$, this is the only theoretically affected isoline function (eqn. (9)). However, given the stator field's weakness compared to that of the rotor, its impact on $\{b_{\max}, b_{\min}\}$ may be considered negligible.

Based on the reviewer's comment and the above discussion, the following changes were made to the manuscript:

- Supplementary Material: Added a new supplementary figure S6 (shown below) quantifying sensor noise signal and the stator field compared to the rotor.
- Results (line 192-198): Added a paragraph containing the above reasoning why the magnetic field of the stators is ignored in formulation of the isoline functions used for localizations.
- Discussion (line 391-392): Added that the stator field is considered negligible, as its strength is one to two orders weaker than the rotor field.

3. *Typical magnetic localization uses nonlinear optimization or state estimation based on a straight-forward magnetic measurement model to acquire pose estimation. This article, however, analyzes the rotation process using rotor field isoline functions and fits isoline functions for key variables ${}^{\text{S}}\beta$, ${}^{\text{S}}\boldsymbol{p}_{\text{e}}$, and ${}^{\text{S}}\alpha$, which could be a unique contribution of this work. It would be beneficial to further discuss how this parameterization and function fitting benefit the system, as well as how this algorithm compares to conventional methods in other rotating dipole systems. Additionally, the tracking errors in this system appear to be slightly larger than those observed in similar rotating dipole localization systems, and this system has a smaller workspace. Is the algorithm responsible for this discrepancy?*

Response: We thank the reviewer for suggesting to highlight the contribution of introducing the rotor field isoline functions. This requires a comparison to other localization algorithms. Indeed, different magnetic localization methods exist depending on magnetic field characteristics (e.g., stationary, oscillating, rotating), localization of the field source (e.g., internal or external), as well as count, type, and combination of sensors (e.g., magnetometer, accelerometer).

To our knowledge, this paper is the first to report localization of a rotating dipole with perpendicular axes of rotation and magnetization, using a single sensor. Similar algorithms to the one reported exist to localize a single sensor based on the known temporal configuration of a rotating dipole [A][B]. However, in our reverse case, while similarly having access to field measurements, we have no information about the dipole rotation axis. This information is compensated for by formulating predetermined maps between rotating

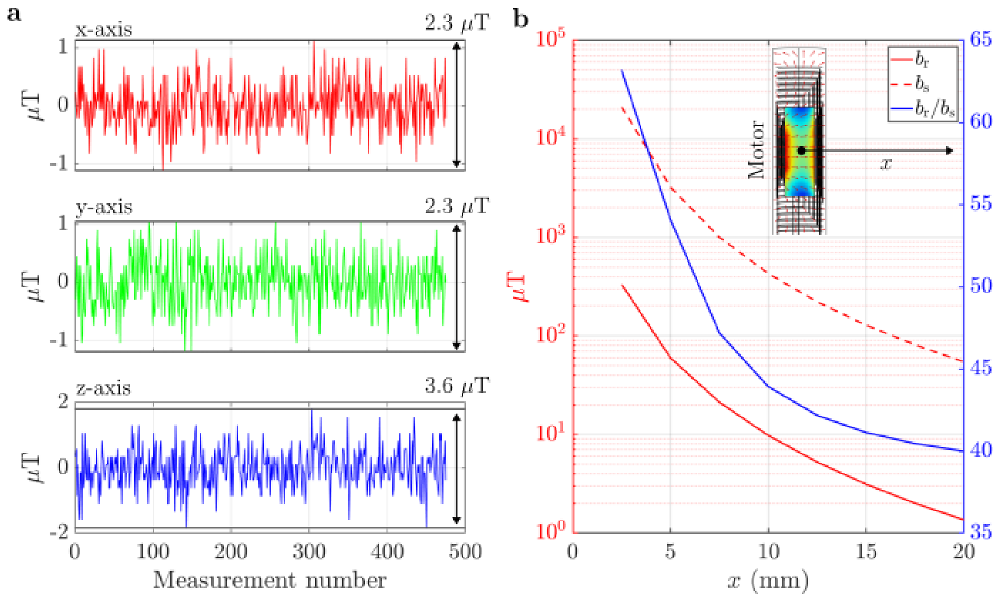

Fig. S6: **Hall effect sensor noise and comparison between magnetic fields of the rotor and stator. a** Noise signal of the Hall effect sensor obtained from a mean-correction of static background field measurements. **b** Finite element simulated magnetic fields of the permanent magnet rotor (b_r) and electromagnet stator (b_s), corrected for driving current (200 mA). In addition, the ratio between rotor and stator fields (b_r/b_s) is shown.

field components and the field source, i.e. the isoline functions.

The localization workspace depends on the signal-to-noise ratio (SNR) of the rotor field measurement. The SNR is influenced by rotor size (magnetic moment) and sensor resolution and noise. Here, the tri-axial Hall effect sensor has 5 mT measurement range, $\sim$ 3 µT peak noise (Supplementary Fig. 6), and 0.1 µT resolution. Accordingly, the workspace was limited 40 mm distance from the sensor. While this workspace is smaller than those using larger magnets [A][B] or more precise sensors [C][D], simulations suggest that reducing sensor noise could extend the workspace beyond 200 mm (Supplementary Fig. 10).

Based on the reviewer's comment and the above discussion, we have made the following changes to the manuscript:

- Discussion (line 356-361): Added a paragraph including the above discussion about introducing isoline functions to localize a rotating dipole with a single sensor.
- Discussion (line 375-376): Added information about our Hall effect sensor's measurement range, noise, and resolution.
- Discussion (line 379-381): Added the comparison of our workspace to those in works [A][B][C][D] and noted that simulations suggest that reducing sensor noise could extend our workspace similarly beyond 200 mm.

[A](32) Popek, K. M., Mahoney, A. W. & Abbott, J. J. Localization method for a magnetic capsule endoscope propelled by a rotating magnetic dipole field. In 2013 IEEE Int. Conf. Robot. Autom., 5348–5353 (IEEE, 2013).

[B](38) Popek, K. M., Schmid, T. & Abbott, J. J. Six-degree-of-freedom localization of an untethered magnetic capsule using a single rotating magnetic dipole. IEEE Robot. Autom. Lett. 2, 305–312 (2016).

[C](36) Fischer, F., Gletter, C., Jeong, M. & Qiu, T. Magneto-oscillatory localization for small-scale robots. NPJ Robot. 2, 1 (2024).

[D](35) Gleich, B., Schmale, I., Nielsen, T. & Rahmer, J. Miniature magneto-mechanical resonators for wireless tracking and sensing. Science 380, 966–971 (2023).

4. *In Figure 6, the position estimation results show a large error peak when the position angle $\beta > 70°$. This is a*

well-known phenomenon in single magnetic source systems, often referred to as a singularity or low-sensitivity issue, as reported in [1] [2]. The article could benefit from referencing these relevant works. However, the error peaks around $\beta = 23°$ is not well-discussed. Considering the system's operating scenario, $\beta \approx 23°$ is a commonly encountered workspace, and significant orientation error (error in ω_{m}) should be discussed in more details.

[1] A. Z. Taddese, P. R. Slawinski, M. Pirotta, E. De Momi, K. L. Obstein, and P. Valdastri, "Enhanced real-time pose estimation for closed-loop robotic manipulation of magnetically actuated capsule endoscopes," The International Journal of Robotics Research, vol. 37, no. 8, pp. 890–911, Jul. 2018

[2] Y. Shen, S. Dong, D. Liu, K. Zhang, and H. Wang, "Active 6-DoF Electromagnetic Pose Tracking Using Orientation Control of the Magnetic Source," 2023 IEEE International Conference on Robotics and Biomimetics (ROBIO), Koh Samui, Thailand: IEEE, Dec. 2023, pp. 1–7.

Response: We appreciate the reviewer's suggestion to include an extended analysis on the localization errors, as well as providing two relevant publications. Indeed, the sensitivity of localization error to field measurement errors varies depending on the region around the rotor magnet [1][2].

Regarding our obtained angular errors in ${}^{\mathrm{S}}\hat{\boldsymbol{p}}_{\mathrm{m}}$ and ${}^{\mathrm{S}}\hat{\boldsymbol{\omega}}_{\mathrm{m}}$, consider that both equally depend on those in reconstructed field vectors $(\{{}^{\mathrm{S}}\hat{\boldsymbol{b}}_{\min}, {}^{\mathrm{S}}\hat{\boldsymbol{\omega}}_{\mathrm{b}}\})$, seen in the governing localization equations (Fig. 5d and eqns. (11)-(13)). Further, ${}^{\mathrm{S}}\hat{\boldsymbol{p}}_{\mathrm{m}}$ depends on ${}^{\mathrm{S}}\alpha$, whereas ${}^{\mathrm{S}}\hat{\boldsymbol{\omega}}_{\mathrm{m}}$ depends on $\{{}^{\mathrm{S}}\beta, {}^{\mathrm{S}}\alpha\}$. Also, ${}^{\mathrm{S}}\alpha$ depends on ${}^{\mathrm{S}}\beta$, that depends on ${}^{\mathrm{S}}b_{\mathrm{ratio}}$. From the partial derivatives of the isoline parameters, we observe that $|\partial\alpha(\beta \leq 60\,°)/\partial\beta| \leq 1$ and mitigates errors in ${}^{\mathrm{S}}\beta$, but amplifies above (new Supplementary Fig. 8, shown below). This is seen from the peaks at $\beta = 23\,°$ and $\beta = 65\,°$ (Fig. 6c(v)-(vi)). Also, $|\partial\beta/\partial b_{\mathrm{ratio}}|$ and $|\partial\alpha/\partial b_{\mathrm{ratio}}|$ are most sensitive to errors at the boundary of $b_{\mathrm{ratio}}(\beta) \in \{1, 2\}$, and least sensitive when $b_{\mathrm{ratio}}(\beta) \in [1.1, 1.9]$. This corresponds to the relative motor-sensor configurations with isoline position angles of $\beta \in [25, 75]\,°$ (Fig. 4f).

Angular errors in $\{{}^{\mathrm{S}}\beta, {}^{\mathrm{S}}\alpha, {}^{\mathrm{S}}\hat{\boldsymbol{p}}_{\mathrm{m}}, {}^{\mathrm{S}}\hat{\boldsymbol{\omega}}_{\mathrm{m}}\}$ expectedly increase with β for which $\|\boldsymbol{b}_{\max} - \boldsymbol{b}_{\min}\|$ falls below the sensor noise and reconstructed components of the measured field become less accurate. Unexpectedly, however, the error $|{}^{\mathrm{S}}\beta - \beta|$ increases linearly with $\beta \leq 23\,°$ (Fig. 6c(v)). This error stems from an overestimation of ${}^{\mathrm{S}}b_{\mathrm{ratio}} \approx 2,\ \forall\beta \leq 23\,°$, which is observed for all field strengths and appears unrelated to the SNR (Fig. 6c(iv)). Therefore, it may be related to a problem with our sensor.

Regarding the 3D tracking experiments in Figure 7, these results support the findings that localization is most accurate for $\beta \in [25, 75]\,°$ (Fig. 6). Angular errors in position vectors are found to be within $\angle\boldsymbol{p}_{\mathrm{m}}, {}^{\mathrm{S}}\boldsymbol{p}_{\mathrm{m}} \in [5, 15]\,°$, whereas for rotation axis within $\angle\hat{\boldsymbol{\omega}}_{\mathrm{m}}, {}^{\mathrm{S}}\hat{\boldsymbol{\omega}}_{\mathrm{m}} \in [10, 40]\,°$. Localization errors increase for $\beta < 25\,°$. Again, possibly due to a region of low sensor accuracy and precision.

Significant errors and deviations in $\angle\hat{\boldsymbol{\omega}}_{\mathrm{m}}, {}^{\mathrm{S}}\hat{\boldsymbol{\omega}}_{\mathrm{m}}$ likely stem from incorrect optimization of the localization coefficients $\{c_1, c_2\}$ (eqn. (14)). Figure 7 (central panels) shows abrupt deviations in the reconstruct position, indicating a series of faulty localizations. These errors persist due to feedback to subsequent localization iterations. Since $\{c_1, c_2\}$ are optimized based on prior positions, the position angular error $(\angle\boldsymbol{p}_{\mathrm{m}}, {}^{\mathrm{S}}\boldsymbol{p}_{\mathrm{m}})$ changes less between iterations. However, an incorrect sign of $c_2 = \pm 1$ already introduces a $90\,°$ error in ${}^{\mathrm{S}}\hat{\boldsymbol{\omega}}_{\mathrm{m}}$ (eqn. (13)), with the potential for significant variation in angular errors $(\angle\hat{\boldsymbol{\omega}}_{\mathrm{m}}, {}^{\mathrm{S}}\hat{\boldsymbol{\omega}}_{\mathrm{m}})$ between iterations.

Based on the reviewer's comment and the above discussion, the following changes were made to the manuscript:

- Figure 6(vi): New subfigure (shown below) regarding error in isoline field angle (α) complementary to the isoline position angle (β) in figure 6(v).
- Supplementary Material: Added a new supplementary figure S7 (shown below) detailing the partial derivatives of the isoline angles $\{\beta, \alpha\}$.
- Results (line 253-261): Added a paragraph on analyzing the angular errors in ${}^{\mathrm{S}}\hat{\boldsymbol{p}}_{\mathrm{m}}$ and ${}^{\mathrm{S}}\hat{\boldsymbol{\omega}}_{\mathrm{m}}$, as discussed above.
- Results (line 264-267): Noted that, unexpectedly, the error $|{}^{\mathrm{S}}\beta - \beta|$ increases linearly with $\beta \leq 23\,°$. That this stems stems from an overestimation of ${}^{\mathrm{S}}b_{\mathrm{ratio}} \approx 2,\ \forall\beta \leq 23\,°$, which is observed for all field

strengths and appears unrelated to the SNR (Fig. 6c(iv)). That, therefore, this error may be related to a problem with our sensor, such as a region of low accuracy and precision.

- Results (280-290): Added paragraphs on the significant tracking errors in ${}^{\mathrm{S}}\boldsymbol{\omega}_{\mathrm{m}}$ due to faulty localizations.
- Discussion (line 362-372): Added paragraphs on the isoline function error sensitivities and identify regions around the rotor where localization is most accurate [1][2]

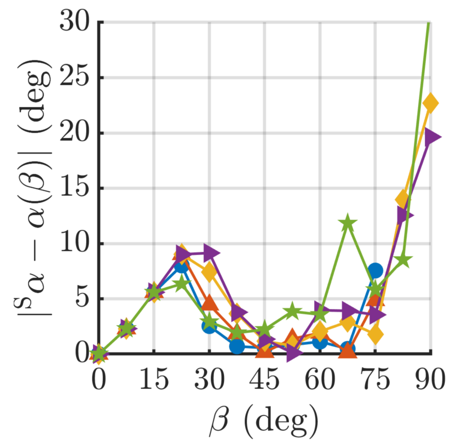

Figure 6: Updated figure 6(vi). Angular error in reconstructed isoline field angle.

5. *In the manipulation and localization experiments, the use of additional tri-axial magnetometers seems acceptable, as the external space is not confined. Adding one to three more magnetometers will help the system determine a unique solution without compromising its compact configuration.*

   Response: We agree that using more tri-axial magnetometers is perfectly feasible with the available space on the external system. This will arguably improve the localization accuracy, and solve the ambiguity problem of reconstructed motor position/rotation axis that is encountered when using one sensor. Accordingly, the following change has been made to the manuscript:

   - Discussion (349-352): Note that the fourfold ambiguity of localization may be resolved using additional sensors mounted on the external manipulation system, enabling localization through triangulation.

6. *Typically, the Hall-effect magnetometer has limitations in terms of sensitivity and resolution, which may impact the system's accuracy. Additionally, the resolution and sensory noise are needed to be listed in the article.*

   Response: The sensor's resolution and noise indeed determine the localization accuracy and workspace. These properties are therefore important to be listed. We have made the following changes:

   - Discussion (line 375-376): Mention the measurement range (5 mT), sensory noise (≈3 µT), and resolution (0.1 µT).
   - Discussion (line 385-386): Note that the localization accuracy is determined by the sensor's signal-to-noise ratio, accuracy, and precision.

7. *The system in this article does not appear to be a strictly simultaneous magnetic manipulation and localization system. Therefore, the phase transition or mode-switching time becomes a critical factor for its efficiency. Are there any modifications that could accelerate this process? Why are sinusoidal currents used to drive the stator coils, given that DC currents would typically provide higher power output, when activating the rotating PM? Additionally, LMPA solidification time should also be experimentally tested and discussed.*

   Response: Indeed, localization and manipulation was performed iteratively rather than simultaneously [A][B]. This was necessary because the external electromagnet's field overpowers the stators, preventing rotor rotation, and saturates the eye-in-hand Hall effect sensor, hindering localization.

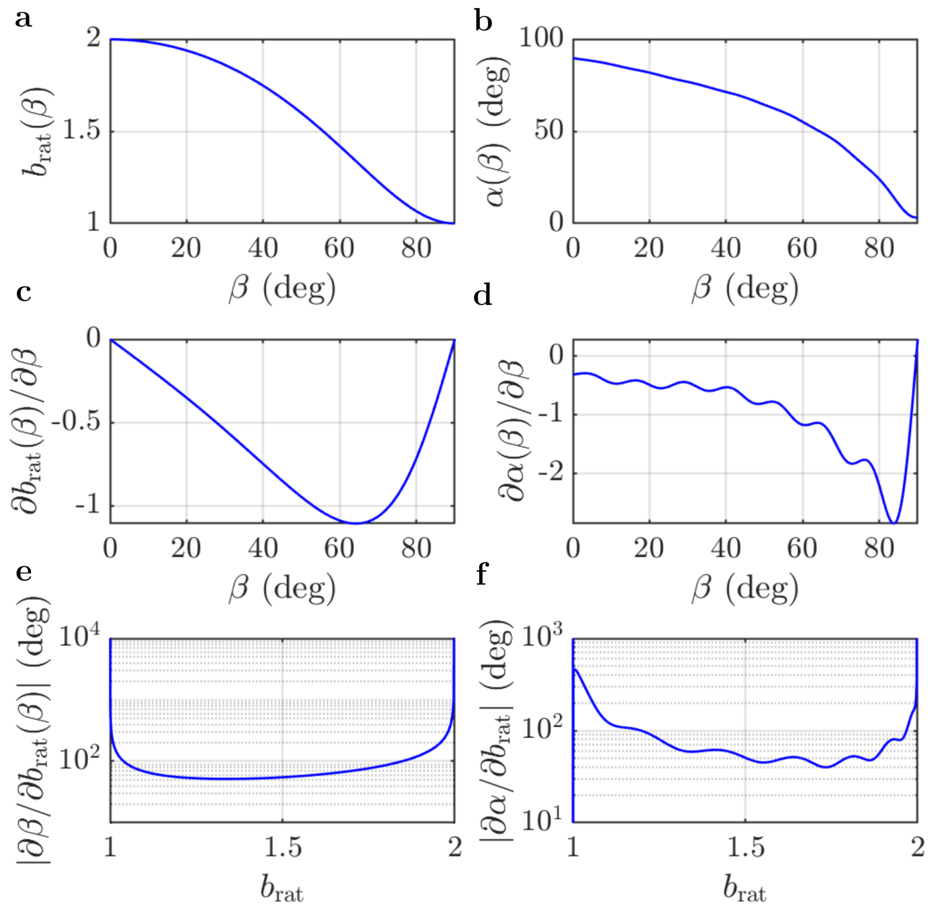

Fig. S 8: **Error sensitivity of the (angular) rotor isoline functions.** **a** Output of the rotor isoline function for field ratio ($b_{\mathrm{rat}}(\beta) := b_{\mathrm{ratio}}(\beta)$) at isoline position angles (β). **b** Output of the rotor isoline function for field angle ($\alpha(\beta)$) at isoline position angles (β). **c** Gradient of $b_{\mathrm{ratio}}(\beta)$ with respect to β. **d** Gradient of $\alpha(\beta)$ with respect to β. The oscillatory profile is due to the sinusoidal function (eqn. (6) of main text) that is fit to $\alpha(\beta)$. **e** Error sensitivity of β with respect to field ratio: $\partial\beta/\partial b_{\mathrm{rat}} = 1/(\partial b_{\mathrm{rat}}/\partial\beta)$. **f** Error sensitivity of α with respect to field ratio: $\partial\alpha/\partial b_{\mathrm{rat}} = (\partial\alpha/\partial\beta)\cdot(\partial\beta/\partial b_{\mathrm{rat}})$.

The rate of mode-switching depends on the time to liquefy or solidify the alloy as a result of resistive heating or passive cooling of the motor, respectively. The previous manuscript included temperature measurements during only the heating phase. This temperature was shown to be related to the time for the LMPA to liquefy and rotor to start rotating.

To identify LMPA solidification time, we have repeated temperature experiments to include the cooling phase (switching off the current). Indicative from these new measurements, the heating phase is the primary bottleneck for rapid switching. Specifically, heating phase steady-state temperature is reached in 20 s in water and 45 s in air, while passive cooling below the LMPA transition temperature takes 2 s in both cases. The heating process could be accelerated using larger initial stator driving currents with electrical resistance-based temperature feedback [C].

Regarding the motor design and profile of driving currents, the manuscript describes localization of a rotating magnetic dipole. Hence, the motor was equipped with a permanent magnet rotor and a stationary electromagnet stator. To the authors' knowledge, this constitutes a permanent magnet synchronous motor (PMSM). A PMSM uses AC current through the stators to generate a rotating magnetic field that interacts with the rotor. This approach is inspired by, and reported in, other works that report milli-scale PMSMs [D][E][F]. However, we think that a discussion on AC and DC motors is beyond the scope of our manuscript.

Based on the reviewer's comment and the above discussion, the following changes were made to the manuscript:

- Discussion (line 402-403): Noted that magnetic manipulation and localization was performed iteratively rather than simultaneously [A][B].
- Supplementary Figure 3 (shown below): Updated figure to show setup for new temperature measurements in both air (18degC) and water (37degC).
- Figure 3c (shown below): Updated subfigure to show internal and external temperature response to quadrature currents during both the heating and cooling phase.
- Results (line 118-126): Updated results to include temperature measurements in water and cooling phase.
- Discussion (line 336-342): Included discussion on heating and cooling times with the relation to rate of mode-switching.
- Discussion (line 342-344): Noted that rate of mode-switching is limited by the heating phase, which may be accelerated using elevated initial stator driving currents with electrical resistance-based temperature feedback [C].

[A](30) von Arx, D. et al. Simultaneous localization and actuation using electromagnetic navigation systems. IEEE Trans. Robot. 40, 1292–1308 (2023).

[B](60) Popek, K. M., Hermans, T. & Abbott, J. J. First demonstration of simultaneous localization and propulsion of a magnetic capsule in a lumen using a single rotating magnet. In 2017 IEEE Int. Conf. Robot. Autom., 1154–1160 (IEEE, 2017).

[C](59) Mattmann, M. et al. Thermoset shape memory polymer variable stiffness 4d robotic catheters. Adv. Sci. 9, 2103277 (2022)

[D](50) Wang, T. et al. Development of a high-speed synchronous micro motor and its application in intravascular imaging. Sens. Actuator A Phys. 218, 60–68 (2014).

[E](47) Assadsangabi, B., Tee, M. H., Wu, S. & Takahata, K. Catheter-based microrotary motor enabled by ferrofluid for microendoscope applications. J. Microelectromech. Syst. 25, 542–548 (2016)

[F](48) Jayhooni, S. M. H., Assadsangabi, B. & Takahata, K. A stepping micromotor based on ferrofluid bearing for side-viewing microendoscope applications. Sens. Actuator A Phys. 269, 258–268 (2018).

8. *Is there a specific design in place to prevent the liquidized alloy from leaking? While the article discusses the safety of the LMPA melting temperature, it would be helpful to briefly address the design considerations for preventing leaks and potential hazards associated with the LMPA to the human body.*

Response: The final step of the motor's fabrication process includes encapsulation by a resin shell that prevents leakage of the alloy. Encapsulation of the alloy is necessary for medical applications due to it containing toxic elements [A].

Accordingly, the following changes were made to the manuscript:

- Results (line 97-98): Noted that a resin shell/seal prevents leakage of alloy.
- Discussion (line 334-335): Noted that due to the liquid state and toxic elements of Cerrolow-117, the motor requires encapsulation for medical applications [A].
- Methods (line 475): mention that the dip coating of the motor also prevents leakage of alloy during activation.

[A](53) Chautems, C. et al. Magnetic continuum device with variable stiffness for minimally invasive surgery. Adv. Intell. Syst. 2, 1900086 (2020).

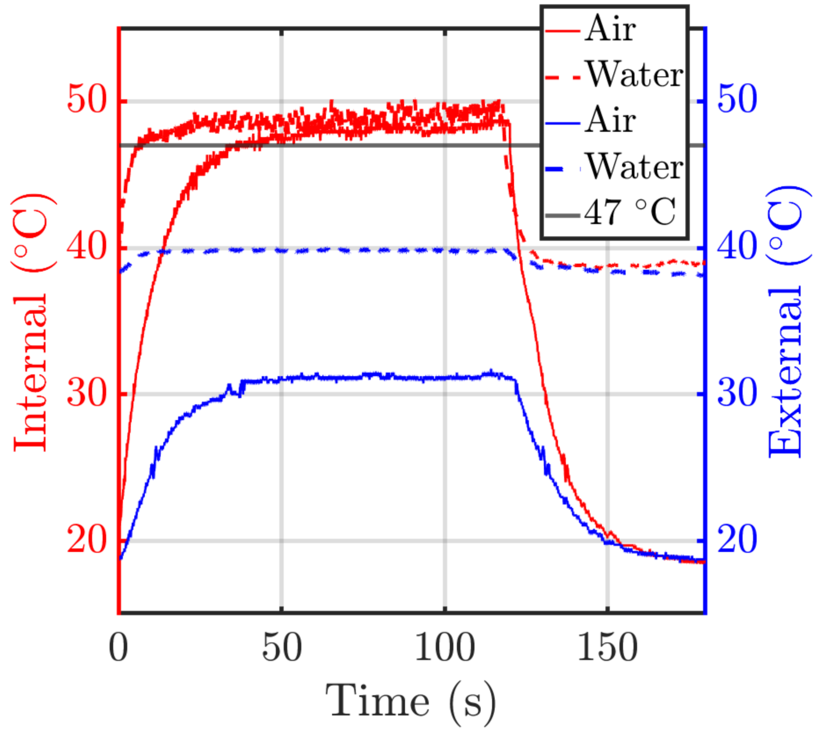

Figure 3: Updated figure 3c. Measured internal and surface temperatures from 200 mA quadrature currents in room-temperature air (18 °C) and heated water (37 °C)

Reviewer 3

I found this to be a quite interesting paper and design concept/paradigm. The authors make a kind of robotic guidewire that effectively has a tiny brushless motor in its tip. Using this motor, they can rotate the permanent-magnet rotor via the electromagnetic stator, and then pick up this rotating dipole field using Hall-effect sensors (which would be located outside of the patient's body in practice). This localization is used while traversing vasculature. Since the Hall-effect sensors are on a system outside of the body, it is reasonable to assume that the Earth's magnetic field can be calibrated away, enabling measurement of very small fields. If magnetic steering is needed, such as to select a branch at a given branch point, then a ferrofluid bearing is allowed to solidify, stopping the rotating-magnet localization function, but enabling traditional magnetic-tip steering using an external magnetic-actuation system (which is now being done blind, but over a tiny workspace). Once steering is complete, the ferrofluid is melted using induction (using the same stator coils) and the rotating-magnet localization can begin again. The authors include a number of clarifying videos that help the reader understand what is happening.

Response: We thank the reviewer for their evaluation of the manuscript, and are pleased they find it interesting.

There is a lot of prior work on doing localization using rotating magnetic dipole fields. I find the literature search largely sufficient. However, it is often unclear what developments regarding localization using rotating magnetic dipoles are newly developed here, and what has already appeared in the literature. References to the literature are largely isolated to the Introduction. Also, there are two uncited papers that are also about localization using a rotating magnetic dipole (although, by contrast, the place sensors inside the body):

Response: We thank the reviewer for listing two relevant papers [B][C] that should be added to the references. Also, we agree that more discussion should be given on the novelty of the localization algorithm, with reference to other works based on rotating dipoles.

The primary development regarding localization using rotating magnetic dipoles are the the isoline functions.

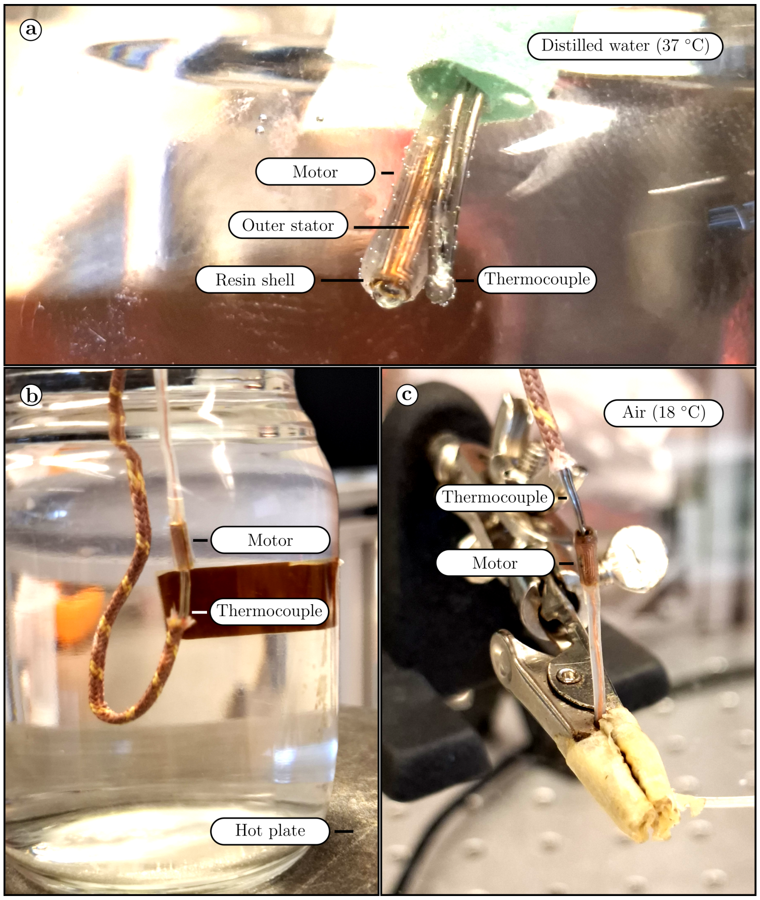

Fig. S3: **Temperature measurements. a** External temperature measurement inside a bath of distilled water at 37 °C. Visible are the motor with outer stator and resin shell, but without the permanent magnet rotor, and a thermocouple placed along its outer surface. **b** Internal temperature measurement inside a bath (glass jar) of distilled water at 37 °C. The thermocouple is placed inside the motor's rotor cavity. The water is heated with a hot plate. **c** Internal temperature measurement inside air at 18 °C.

The presented algorithm localizes a PMSM, modeled as a magnetic dipole with perpendicular rotation and magnetization axes. At its core, the algorithm uses precomputed rotor field isoline functions (eqns. (4)-(6)) that link rotating field properties to the rotating field source (Fig. 4d) and Supplementary Fig. 5). By computing a ratio (b_{ratio}) of maximum and minimum field strengths ($\{b_{\max}, b_{\min}\}$) at a given position, the algorithm determines a set of isoline angles ($\{\beta, \alpha\}$) to rotate the measured field's rotation axis ($\hat{\boldsymbol{\omega}}_{\mathrm{b}}$) into four possible combinations of dipole position and rotation axis ($\{\hat{\boldsymbol{p}}_{\mathrm{m}}, \hat{\boldsymbol{\omega}}_{\mathrm{m}}\}$) (eqns. (8)-(10)).

This fourfold ambiguity is also reported in previous work [A]. Herein, this is resolved using prior knowledge of dipole position. However, this method risks forwarding of a previous faulty localization (Fig. 7). To prevent this, additional sensors may be mounted on the external manipulation system, enabling localization through triangulation.

Supporting the formulation of the isoline functions, we note that similar algorithms exist to localize a sensor based on the known temporal configuration of a rotating dipole [A][B][C]. However, in our reverse case, while similarly having access to field measurements, we have no information about the dipole rotation axis. This information is compensated for by formulating predetermined maps between rotating field components and the field source, i.e. the isoline functions.

As an additional contribution, the isoline functions may be used to analyze motor-sensor configurations at which the localization accuracy is most sensitive to field measurement errors. To this end, we define a so called "isoline error sensitivity" that describes how errors in measured field ratio (${}^{\mathrm{S}}b_{\mathrm{ratio}}$) affect errors in the isoline angles ($\{^{\mathrm{S}}\beta, {}^{\mathrm{S}}\alpha\}$). A new analysis of partial derivatives indicate that $\partial\beta/\partial b_{\mathrm{ratio}}$ is least sensitive for $b_{\mathrm{ratio}} \in [1.1,\ 1.9]$, corresponding to $\beta \in [25, 75]\ ^{\circ}$ (new Supplementary Fig. 8, shown below). Further, $|\partial\alpha/\partial\beta| \leq 1,\ \forall\beta \in [0, 60]\ ^{\circ}$ corresponding to $b_{\mathrm{ratio}} \in [1.4, 2]$, mitigates errors in ${}^{\mathrm{S}}\beta$ but amplifies above. Overall, this suggests that PMSM directionality vectors $\{^{\mathrm{S}}\hat{\boldsymbol{p}}_{\mathrm{m}}, {}^{\mathrm{S}}\hat{\boldsymbol{\omega}}_{\mathrm{m}}\}$ are least sensitive to reconstruction errors in b_{ratio} for relative rotor-sensor positions at $\beta \in [25, 60]\ ^{\circ}$, for which $b_{\mathrm{ratio}} \in [1.4, 1.9]$.

Based on the above discussions following the reviewer's comment, we have made the following changes to the manuscript:

- Discussion (line 345-351): Added paragraphs to describe the workings of the isoline functions, compare the fourfold ambiguity in the localization solution to similar works [A], and argue the development of isoline functions to compensate missing information of a rotating dipole axis [A][B][C].
- Discussion (line 362-372): Added a paragraph about the error sensitivity of the localization algorithm to field measurement errors at different relative motor-sensor positions.
- Supplementary Material: Composed a new supplementary figure 8 (shown below) regarding gradients of the isoline angles.

[A](32) Popek, K. M., Mahoney, A. W. & Abbott, J. J. "Localization method for a magnetic capsule endoscope propelled by a rotating magnetic dipole field." In 2013 IEEE Int. Conf. Robot. Autom., 5348–5353 (IEEE, 2013).

[B](38) Popek et al.,, "First Demonstration of Simultaneous Localization and Propulsion of a Magnetic Capsule in a Lumen using a Single Rotating Magnet", IEEE International Conference on Robotics and Automation, pp. 1154-1160, 2017.

[C](61) Sperry et al., "Six-degree-of-freedom Localization with a 3-axis Accelerometer and a 2-axis Magnetometer for Magnetic Capsule Endoscopy", IEEE Robotics and Automation Letters, 7:2110-2115, 2022.

Early in the paper, the authors mention that it is not possible to uniquely localize a rotating magnetic dipole (i.e., the 3-dof position and the axis of rotation) using a single tri-axial Hall-effect sensor, and one can only narrow it down to four possible locations. But then later, they seem to show a unique localization. This discrepancy is only resolved at the end of the paper. My suggestion would be to clarify this earlier in the paper, so the reader isn't left hanging and dwelling on this.

Response: We thank the reviewer for the recommendation and made the following changes to clarify:

- Introduction (line 60-62): Noted that in this work, ambiguity of dipole location is resolved using closed-loop position feedback.
- Results (line 190-191): Noted that in this work, ambiguity in the isoline position angle (β) is resolved using a-priori knowledge of rotor position through closed-loop feedback of previous localizations.
- Discussion (line 352-355): Recite ambiguity and solving with a-priori knowledge. Noting that this method risks forwarding a previous faulty localization. Propose a solution of adding additional sensors that permits triangulation.

One problem that I have with this paper is that it is not very constructive. If I wanted to apply this method to my own problem, it would take substantial effort to reconstruct it. The authors provide all of the pieces, but don't really connect the dots very well. Figure 5 is close to what I'm looking for. Maybe the authors could expand on that content in a narrative fashion (even in Supplementary Material).

Response: We thank the reviewer for the suggestion to clarify the localization algorithm. Indeed, the formulation of rotor field isoline functions, measurement post-processing, and online computation are spread throughout the manuscript. This could benefit from a flow diagram that details the different steps in the localization algorithms. Accordingly, the following changes were made to the manuscript:

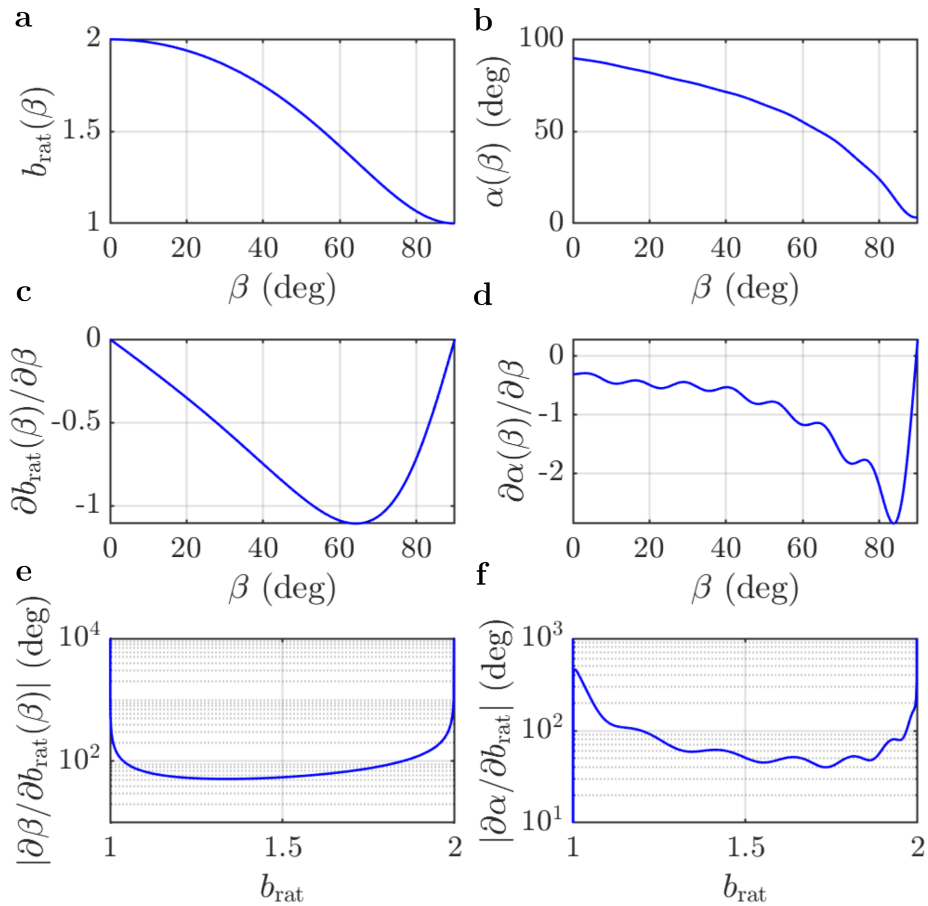

Fig. S 8: **Error sensitivity of the (angular) rotor isoline functions. a** Output of the rotor isoline function for field ratio ($b_{\text{rat}}(\beta) := b_{\text{ratio}}(\beta)$) at isoline position angles (β). **b** Output of the rotor isoline function for field angle ($\alpha(\beta)$) at isoline position angles (β). **c** Gradient of $b_{\text{ratio}}(\beta)$ with respect to β. **d** Gradient of $\alpha(\beta)$ with respect to β. The oscillatory profile is due to the sinusoidal function (eqn. (6) of main text) that is fit to $\alpha(\beta)$. **e** Error sensitivity of β with respect to field ratio: $\partial\beta/\partial b_{\text{rat}} = 1/(\partial b_{\text{rat}}/\partial\beta)$. **f** Error sensitivity of α with respect to field ratio: $\partial\alpha/\partial b_{\text{rat}} = (\partial\alpha/\partial\beta)\cdot(\partial\beta/\partial b_{\text{rat}})$.

- Supplementary Material: Added a new supplementary figure 7 (shown below) that contains a flow diagram of the structure of the localization algorithm, including offline computed isoline functions, inputs, online computation steps, and output. Within the flow diagram, references to equation numbers of the manuscript are given.
- Results (line 204): Added reference to the new Sup. Fig. 7.
- Discussion (line 348): Added reference to the new Sup. Fig. 7.

When the magnetic tip is solidified, the magnetization is diametric (not axial), but I guess it can assumed to be known (at least approximately) based on the last stator commands. However, the localization of the stator, in the roll direction, is likely poorly known, as with all of this type of long, continuum device. I was left wondering how that affected the subsequent steering. For example, I could imagine that the first time the external electromagnet is turned on, it would be difficult to even anticipate what direction the tip would bend in, and it would be almost random. Can you please clarify this aspect of the method.

Response: We thank the reviewer for the suggestion to clarify the method of magnetic manipulation. Indeed, due to the unknown radial orientation of the PMSM magnetic moment, initial application of a manipulation field causes deflection in an indeterminate plane.

As a hypothetical solution, if the rotor rotates synchronously with the stator's sinusoidal field, frequency analysis and sinusoidal fitting of field measurements could produce a time-dependent cyclic function. This function could then be used to predict the temporal direction of the motor's (electro)magnetic moment, which in turn could be used to determine its plane of deflection when an external magnetic field is applied.

Based on the reviewer's comment and the above discussion, the following changes were made to the manuscript:

- Discussion (line 402-415): Added a paragraph regarding magnetic manipulation. This paragraph discusses the iterative approach to magnetic manipulation and localization due to sensor saturation. It also highlights the limitations of the current system with random deflection, suggests improvements through electromagnet field modeling, and proposes frequency analysis as a method to predict the plane of deflection for synchronous motors.

I like the "future work" suggestion that this device could be used as an in-vivo rotating dipole field source. That's an interesting idea.

Response: We are glad that the reviewer finds this idea interesting and hope it may inspire new research.

I was left with questions of scalability. For the device to get even a little smaller, the fabrication of the stator would become more difficult, and probably more importantly, the permanent-magnet rotor would decrease in size, and its field (which is proportional to its volume) would decrease drastically, maybe below the point of being measurable by external Hall-effect sensors. Maybe this device is already small enough for useful tasks?

Response: The manual fabrication process of the PMSM did introduce functional inconsistencies between prototypes. Further miniaturization would likely involve a more consistent automated process, are include precise micro-fabricated parts that (only) require assembly [A].

The size of the magnet does affect the signal-to-noise ratio (SNR) at some distance from a sensor. We previously identified a minimum SNR of 10 dB for localization. For sensor (5 mT measurement range, 3 uT peak noise, 0.1 uT resolution) and our magnet (cylinder, 1 mm diameter, 3 mm length) this limited the workspace to 40 mm. The magnetic moment and field of a permanent magnet scales linearly with its volume. Thus indeed, even smaller magnets would require every increasingly accurate and precise sensors. Accordingly, we have made the following changes to the manuscript:

- Discussion (327-329): Noted that manual fabrication introduced functional inconsistencies. Also, that precise micro-fabricated parts should be considered for reliability and miniaturization [A].
- Discussion (line 374-376): Mentioned the measurement range, peak noise, and resolution of our Hall effect sensor. Also, that the SNR is influenced by rotor size (magnetic moment).
- Discussion (385-386): Noted that localization accuracy is influenced by the sensor's SNR, accuracy, and precision.

[A](50) Wang, T. et al. Development of a high-speed synchronous micro motor and its application in intravascular imaging. Sens. Actuator A Phys. 218, 60–68 (2014).

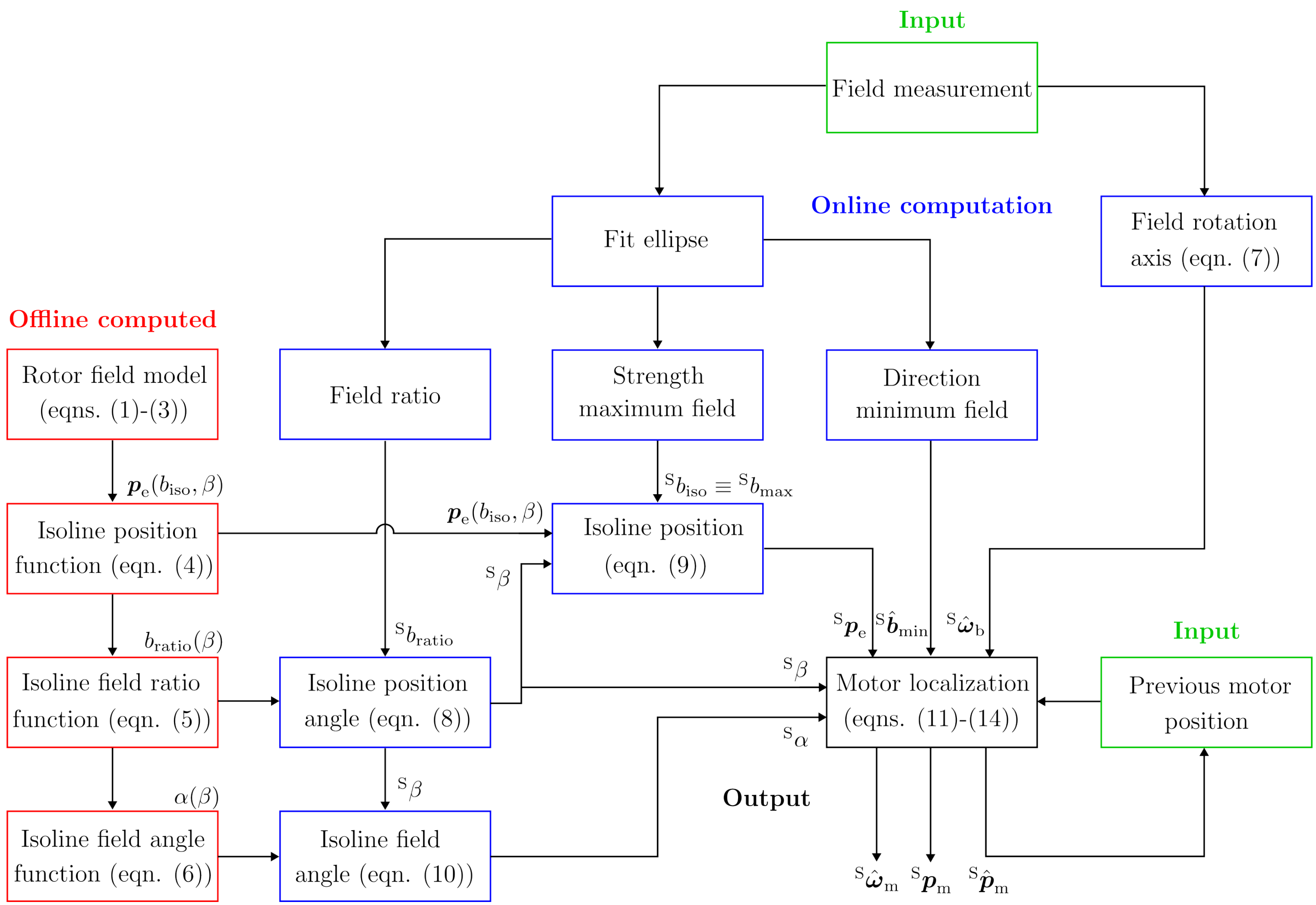

Fig. S7: **Flow diagram of the localization algorithm.** Offline computed rotor field isoline functions are used in conjunction with field measurements to provide online estimations of the motor's position and rotation axis.

Authors' response to the reviewers' comments (round 2)

Manuscript ID: COMMSENG-24-0654A

Magnetic Localization and Manipulation of Locking Synchronous Motors

Authors: Michiel Richter, Lukas Masjothusmann, Pavlo Makushko, Venkatasubramanian Kalpathy Venkiteswaran, Denys Makarov, Sarthak Misra

Reviewer 1

The authors have revised the manuscript according to the reviewers comments. The paper is ready for publication.

Response: We thank the reviewer for accepting our revisions and recommendation for publication.

Reviewer 2

Thank you for your detailed responses. The issues raised in my previous comments have been well addressed with satisfactory revisions. I recommend the publication of this paper after incorporating the following minor comments.

Response: We thank the reviewer for accepting our revisions and appreciate the additional minor comments.

1. *For the previous comment 4 about Figure 6 and experimental results, I appreciate the detailed and sound error analysis provided for the unexpected errors occurring at $\beta \leq 23°$. While I understand the cause of this unexpected error is complicate and difficult to isolate, a hypothesis on the potential cause would be useful and could help enlighten readers. However, regarding the statement in line 266-267 "Therefore, it may be related to a problem with our sensor...", It's not clear how the general sensor problem is directly linked to regional low accuracy. I would suggest reconsidering this claim, either by removing it or providing a more thorough explanation.*

   Response: We thank the reviewer on questioning the hypothesis that a general sensor problem may cause a regional low accuracy, opposed to a global one. This prompts us to rethink this hypothesis.

   Previously, we recognized that the difference between maximum and minimum field strengths must be greater than the sensor noise ($\|\boldsymbol{b}_{\max}\| - \|\boldsymbol{b}_{\min}\| \geq 2$ μT) to be reliably differentiated. We think that logically, by extension, the rate of difference between field strengths $\partial(\|\boldsymbol{b}_{\max}\| - \|\boldsymbol{b}_{\min}\|)/\partial\beta$ must also be "large enough" to be able to distinguish $b_{\text{ratio}}(\beta)$ from $b_{\text{ratio}}(\beta + \Delta\beta)$. Therefore, a potential cause for the unexpected errors at $\beta \leq 23$ ° may indeed not be due to the sensor. Instead, we observe that $\partial(\|\boldsymbol{b}_{\max}\| - \|\boldsymbol{b}_{\min}\|)/\partial\beta \approx 0$, $\forall\beta \leq 23$ ° indicates a region where changes in relative maximum and minimum field strengths are indistinguishable by the sensor (Fig. 6c(iii)).

   - Results (line 267-269): Removed the claim about a general sensor problem.
   - Results (line 267-269): Added the above explanation about a region $\beta \leq 23°$ where changes in relative maximum and minimum field strengths are indistinguishable.

2. *Regarding the previous comment on the use of sinusoidal currents to drive the stator coils in the heating process (previous comment 7), I understand PMSM use AC current to generate the rotating magnetic field. I was wondering about the potential of using DC current exclusively during the heating process (e.g. 0-30s in Fig. 3 (g)) to accelerate the melting process, enhancing the real-time performance of the system. I guess that it is because switching to DC current in heating process requires more complex power circuit design.*

   Response: Thank you for clarifying the previous comment. DC currents can indeed be used during the heating process. However, the duration of heating ultimately depends on power dissipation by the stators. In theory, using either DC currents or higher AC currents–provided they result in the same average power dissipation–should give the same melting duration. An advantage of AC currents is the dual use for both melting and rotor rotation.

- Discussion (line 345-348): Added a paragraph describing that heating time during the rotor unlocking phase depends on power dissipation by the stators, which act as resistors. This process may be accelerated through a greater heat transfer rate, by increasing power dissipation with higher peak currents in the AC signal.

Reviewer 3

I am satisfied with the authors' improvements to the manuscript. They haven't solved every problem yet, but this paper makes an interesting contribution to the literature.

Response: We thank the reviewer for accepting our revisions and recommendation for publication.